Coherent population trapping in a Λ configuration coupled by magnetic dipole interactions

Huidong Kim, Hyok Sang Han, Tai Hyun Yoon, and D. Cho[*]

Department of Physics, Korea University, Seoul 136-713, Korea
(Received 6 January 2014; published 10 March 2014)

We report our study on coherent population trapping (CPT) in a Λ configuration coupled by magnetic dipole interactions. The Λ configuration is formed by bichromatic radio-frequency fields coupling a pair of Zeeman sublevels in one hyperfine level of an alkali-metal atom to another sublevel in the other hyperfine level. The Zeeman sublevel at the apex is coupled to a state in the nP manifold via an optical transition on one of the spectroscopic D lines to induce optical pumping to a dark state. The configuration is closed without leakage to other Zeeman sublevels. We use lithium atoms in an optical trap for our experimental study. The system allows independent control of the main parameters characterizing CPT, which include the upper-state decay rate and the decoherence rate as well as the Rabi frequencies. By turning off the applied fields, the system is frozen so that its quantum state can be measured precisely. We studied the line shapes and dynamics of the CPT system, and measured the phase relation of the dark superposition state to find excellent agreement with theory. The possible application of the scheme as a method to cool optically trapped atoms below the recoil limit in a manner analogous to velocity-selective coherent population trapping is discussed.

I. INTRODUCTION

Coherent population trapping (CPT) [1] has been studied both theoretically and experimentally from diverse perspectives [2,3]. Its narrow resonance has led to the development of compact atomic clocks [4] and highly sensitive magnetometers [5]. The steep dispersion accompanying the CPT transmission window allowed significant reduction in the group velocity of a light pulse [6]. The phenomenon has also been used to enhance nonlinear optical signals [7] and to cool atoms below the recoil limit by velocity-selective coherent population trapping (VSCPT) [8].

An alkali-metal atom with a pair of ground hyperfine levels and a strongly coupled excited state provides a Λ system well-suited for CPT. Although various scenarios have been considered, bichromatic light fields to drive the D transitions via electric dipole ($E1$) interactions have formed the backbone of the Λ configuration without exception. In this paper, we report our study on CPT driven by magnetic dipole ($M1$) interactions. We consider a Λ system consisting of a pair of Zeeman sublevels $|1\rangle,|2\rangle$ in one hyperfine level and another sublevel $|3\rangle$ in the other hyperfine level coupled by a pair of radio-frequency (rf) fields. However, this system alone cannot exhibit CPT because while CPT is an optical pumping process via spontaneous decay of the upper state, the $|3\rangle$ state is virtually stationary. This can be remedied by adding an optical field $\vec{E}_c$ coupling $|3\rangle$ to a state $|4\rangle$ belonging to the nP manifold as shown in Fig. 1(a). The resulting "inverted Y" configuration [9] can be reduced to an effective CPT Λ configuration as shown below. In our experiment, we use optically trapped ^{7}Li atoms [Fig. 1(b)]; $|2S_{1/2},F = 2,m_F = -2\rangle$ and $|F = 2,m_F = -1\rangle$ play the roles of $|1\rangle$ and $|2\rangle$, respectively, while $|F = 1,m_F = -1\rangle$ is used for $|3\rangle$, and $|2P_{1/2},F = 2,m_F = -2\rangle$ for $|4\rangle$. F is the total angular momentum and m_F is its z component. Although $|3\rangle$ has a lower energy than $|1\rangle$ or $|2\rangle$, all three states are stable

and the system can be suitably described as an inverted Y configuration.

The experimental situation of our $M1$ CPT has certain unique features that are complementary to $E1$ CPT: (i) While in an $E1$-CPT experiment the coherent properties of a medium are inferred from the transmitted light fields, we cannot use the method because of the large spatial extent and the low detection efficiency of the rf fields. Instead, we can probe the medium itself. Unlike $E1$ CPT, wherein a fast-decaying upper state is a permanent feature, we can turn off $\vec{E}_c$ as well as the rf fields to freeze the quantum state of the medium for subsequent probing. The state of the optically trapped atoms without the driving fields changes slowly and there is sufficient time to measure it accurately. This allows us to monitor the evolution of the system frame by frame and characterize the dark superposition state. (ii) There are three main parameters for CPT: the upper-state decay rate Γ_u, the coherence decay rate γ_{ij} ($i \neq j$), and the Rabi frequencies Ω_p, Ω_q. While Γ_u in $E1$ CPT is fixed as the spontaneous decay rate of the $|nP\rangle$ state, that in our experiment can be varied by adjusting the amplitude of $\vec{E}_c$. We can measure Γ_u from decay of the population in the $|3\rangle$ state while $\vec{E}_c$ is applied. Similarly, we can vary γ_{ij} by introducing a calibrated magnetic-field fluctuation. γ_{ij} and $\Omega_{p,q}$ can be measured by Ramsey and Rabi spectroscopy, respectively. In this manner, we can independently control the three parameters with high precision. (iii) One problem with $E1$ CPT using alkali-metal atoms is that the Λ system is not closed because the upper state $|nP_J,F',m'_{F'}\rangle$ can always decay into ground Zeeman sublevels outside the system. The five-level "inverted W" [10,11] and the four-level double Λ systems [12] can solve this problem only partially in spite of the significantly more complicated experimental situations. In a true steady state of $E1$ CPT, all atoms are pumped out of the Λ system, and CPT is observable in only a transient manner as the atoms move in and out of the laser beams [13]. In contrast, our $M1$-CPT system in Fig. 1(b) is closed, and the atoms experience the same interactions from beginning to end.

In addition to providing an ideal system to study CPT, $M1$ CPT may be used to induce nonlinear optical effects mediated

[*]cho@korea.ac.kr
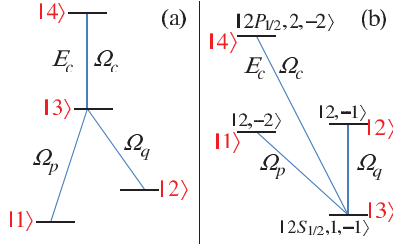
FIG. 1. (Color online) (a) Inverted Y configuration. (b) Realization of the configuration using ^{7}Li atoms.

by $M1$ interactions in the manner that $E1$ CPT has been used to achieve nonlinear effects with low-intensity optical fields [14]. It is also conceivable to use the closed $M1$-CPT system in Fig. 1(b) to cool the vibrational motion of optically trapped atoms beyond the Lamb-Dicke limit in a manner analogous to VSCPT. For a one-dimensional optical lattice formed by a Gaussian standing wave, the Lamb-Dicke parameter η for the longitudinal motion is well below 1 allowing sideband cooling of the motion to the ground vibrational level. In a typical lattice, however, η for the transverse motion is of order 1 or larger, which implies that the recoil limit prevents cooling to the ground level. When $\eta \approx 1$, on the other hand, spontaneous emission can redistribute the vibrational states and it is possible to optically pump the trapped atoms to a CPT dark state under a proper arrangement. When the trapping field is circularly polarized, the potential wells for the two Zeeman states $|1\rangle, |2\rangle$ are different owing to the vector polarizability β [15], and the two-photon resonance condition depends on the motional quantum number n. This dependence can be exploited to optically pump atoms to a dark state with a specific n, for example, $n = 0$, as the velocity dependence of the resonance condition allows pumping to the zero-velocity state in VSCPT. Cooling time required to put atoms in the ground vibration level depends on β and the well depth. For a rubidium or a cesium atom, which has relatively large β, cooling time less than 1 s is expected for a typical lattice when the atoms are precooled by the sideband cooling.

II. THEORY

In order to derive the density matrix equations for the $M1$-CPT system, we start with the inverted Y system in Fig. 1(a). The energy eigenvalue of the $|j\rangle$ state is $\hbar\omega_j$ for $j = 1, 2, 3, 4$. $M1$ transitions are driven by rf fields with $\vec{B}_j(t) = \vec{B}_j e^{-i\omega_j t} + \text{c.c.}$, where $j = p, q$. The Rabi frequencies are $\Omega_p = \langle 3| -\vec{\mu} \cdot \vec{B}_p |1\rangle/\hbar$ and $\Omega_q = \langle 3| -\vec{\mu} \cdot \vec{B}_q |2\rangle/\hbar$, where $\vec{\mu}$ is a magnetic dipole moment operator. $\Delta_p = \omega_p - (\omega_3 - \omega_1)$ and $\Delta_q = \omega_q - (\omega_3 - \omega_2)$ are the single-photon detunings and $\delta = \Delta_p - \Delta_q$ is the two-photon detuning. The coupling field is $\vec{E}_c(t) = \vec{E}_c e^{-i\omega_c t} + \text{c.c.}$ The Rabi frequency is $\Omega_c = \langle 4| -\vec{d} \cdot \vec{E}_c |3\rangle/\hbar$, where $\vec{d}$ is an electric dipole moment operator, and $\Delta_c = \omega_c - (\omega_4 - \omega_3)$ is the detuning. The master equations for an inverted Y system driven by three laser fields were developed in Ref. [9]. In our $M1$-CPT experiment, $\Omega_{p,q}$ and $\vec{E}_c(t)$ are chosen so that the spontaneous decay rate Γ_4 of the $2P$ state is at least five orders of magnitude larger than $\Omega_{p,q}$ and the transition rate R from $|3\rangle$ to $|4\rangle$, where

$R = |\Omega_c|^2 \Gamma_4 / (\Delta_c^2 + \Gamma_4^2/4)$. This allows us to adiabatically eliminate the $|4\rangle$ state and reduce the four-level system to the three-level Λ system. The details are given in the Appendix. The resulting equations for the density-matrix elements ρ_{ij} of the Λ system in the interaction picture are

$$\dot{\rho}_{11} = i\Omega_p(\rho_{13} - \rho_{31}) + p_1 R \rho_{33}, \tag{1a}$$

$$\dot{\rho}_{22} = i\Omega_q(\rho_{23} - \rho_{32}) + p_2 R \rho_{33}, \tag{1b}$$

$$\dot{\rho}_{12} = -i\Omega_p\rho_{32} + i\Omega_q\rho_{13} - (i\delta + \gamma_{12})\rho_{12}, \tag{1c}$$

$$\dot{\rho}_{13} = i\Omega_p(\rho_{11} - \rho_{33}) + i\Omega_q\rho_{12} - (i\Delta_p' + R/2 + \gamma_{13})\rho_{13}, \tag{1d}$$

$$\dot{\rho}_{23} = i\Omega_p\rho_{21} + i\Omega_q(\rho_{22} - \rho_{33}) - (i\Delta_q' + R/2 + \gamma_{23})\rho_{23}. \tag{1e}$$

$\rho_{11} + \rho_{22} + \rho_{33} = 1$ and $\dot{\rho}_{ij} = \dot{\rho}_{ji}^*$ when $i \neq j$. The Rabi frequencies are assumed to be real. $p_1 = 1/6$ and $p_2 = 1/3$ are the branching ratios for the decays from $|4\rangle$ to $|1\rangle$ and $|2\rangle$, respectively. $\Delta_p' = \Delta_p - \delta_3$ and $\Delta_q' = \Delta_q - \delta_3$, where $\delta_3 = |\Omega_c|^2/\Delta_c$ is the ac-Stark shift of the $|3\rangle$ state due to its coupling to $|4\rangle$ by $\vec{E}_c$.

The above equations are essentially the same as those for $E1$ CPT of a Λ configuration [2] except: (i) the spontaneous decay rate Γ_{nP} of the nP state in $E1$ CPT is replaced with the transition rate R, (ii) $p_1 + p_2 = 1 - p_3 < 1$, where $p_3 = 1/2$ is the branching ratio from $|4\rangle$ to $|3\rangle$, and (iii) in $E1$ CPT, γ_{13} and γ_{23} are much smaller than Γ_{nP} and they are usually neglected in Eqs. (1d) and (1e), respectively, but we include them because they can be comparable to R. The total decoherence rate $1/\tau_{ij}$ for optically trapped atoms is contributed by two dephasing mechanisms: $1/T_2^*(ij)$ from inhomogeneous broadening due to thermal distribution of the atoms coupled with a differential ac-Stark shift between the states $|i\rangle$ and $|j\rangle$ [16] and $1/T_2'(ij)$ from homogenous broadening due to magnetic-field fluctuation such that $1/\tau_{ij} = 1/T_2^*(ij) + 1/T_2'(ij)$. We identify γ_{ij} with $1/T_2'(ij)$. The effect of inhomogeneous broadening can be included by convoluting ρ_{ij} with the thermal distribution of the trapped atoms.

III. EXPERIMENT AND RESULTS

The apparatus used in the experiment has been described in our previous publications [17,18]. The relevant features are: ^{7}Li atoms in a magneto-optical trap (MOT) are loaded to an optical trap in a glass chamber placed inside a three-layer magnetic shield. The optical trap is formed by focusing a linearly polarized 6-W laser beam at 1060 nm to a spot with an intensity radius of 20 μm. The well depth is 0.7 mK and 10^4 atoms at 140 μK are trapped in 1 s. Bichromatic rf fields at 803 MHz from a pair of frequency synthesizers, phase locked to a rubidium clock, are fed to a patch antenna underneath the chamber. A 10-μT magnetic field along the trap beam defines the quantization axis. In our study of $M1$ CPT, we measure the populations ρ_{11}, ρ_{22}, and ρ_{33}. Among the three states, only atoms in the $|3\rangle$ state can be magnetically trapped. The trapped atoms are held for 150 ms and transferred to the MOT. MOT fluorescence is imaged onto a photodetector and a phase-sensitive detection is used by modulating the repump frequency to measure the number of atoms in $|3\rangle$ to within

200. For the $|1\rangle$ or $|2\rangle$ state, we apply a π pulse of either Ω_p or Ω_q, respectively, to swap the atoms with those in $|3\rangle$, and we use the same detection method.

We first measure $\Omega_{p,q}$, R, and τ_{ij} to set the CPT parameters. The trapped atoms are optically pumped to the $|1\rangle$ state and Ω_p is determined by observing a Rabi oscillation to $|3\rangle$. Similarly Ω_q is determined using the atoms prepared in the $|3\rangle$ state by the optical pumping followed by a π pulse of Ω_p. In order to measure R, we apply $\vec{E}_c$ to the atoms in $|3\rangle$ for t_c, and measure the remaining fraction, which decays exponentially. The decay time constant τ_3 is related to R as $R = 2/\tau_3$ considering $p_3 = 1/2$. $\vec{E}_c(t)$ is left circularly polarized and blue detuned by 80 MHz to the $|3\rangle$ to $|4\rangle$ transition. Polarization degradation accompanying the coupling-beam delivery via mirrors and lenses can induce parasitic transitions to the $|2P_{1/2}, F = 2, m_F = 0\rangle$ state leading to leakage out of the Λ system. We use a half wave plate in addition to the quarter wave plate to compensate for the degradation [19], and the leakage rate was negligible compared to R. We use Ramsey spectroscopy for the $|i\rangle$ to $|j\rangle$ transition to measure the total decoherence rate $1/\tau_{ij}$. $\rho_{ii}(t)$ follows $[1 + e^{-t/\tau_{ij}} \cos(\Delta\omega t)]/2$, where $\Delta\omega$ is the detuning. Ramsey spectroscopy between $|1\rangle$ and $|2\rangle$ for τ_{12} is difficult because the Zeeman sublevels in the same F state are equally spaced and all pairs of adjacent sublevels are resonant at $\omega_2 - \omega_1$. For a selective transition, we use a stimulated Raman transition (SRT) with the $|3\rangle$ state as an intermediate state by applying both Ω_p and Ω_q. At two-photon resonance, a $\pi/2$ transition between $|1\rangle$ and $|2\rangle$ can be driven without populating other Zeeman sublevels when $\Delta_p = \Delta_q = \Delta$ and $|\Omega_p| = |\Omega_q| = |\Omega|$ satisfy the quantization conditions for a given pulse duration $t_{\pi/2}$,

$$\Delta t_{\pi/2} = (2m + 1)\pi, \tag{2a}$$

$$Z t_{\pi/2} = 2n\pi, \tag{2b}$$

where $Z = \sqrt{\Delta^2 + 8|\Omega|^2}$, m is an integer, and n is a positive integer [18]. We use the simplest mode ($m = 0, n = 1$) for the Raman-Ramsey spectroscopy. With the linearly polarized trapping field, $1/T_2^*(12)$ from inhomogeneous broadening is negligible, and $\tau_{12} \approx T_2'(12) = 650$ ms is mainly due to magnetic-field fluctuation $\delta B(t)$. In this case, $1/\tau_{12}$ is identified to be γ_{12}. For a given $\delta B(t)$, $T_2'(ij)$ is inversely proportional to $(g_F m_F - g_{F'} m'_{F'})^2$ when $|i\rangle = |F, m_F\rangle$ and $|j\rangle = |F', m'_{F'}\rangle$ [17]. We use the relation to estimate $1/\gamma_{13}$ and $1/\gamma_{23}$ to be 650/9 and 650/4 ms, respectively. For the $|1\rangle$ to $|3\rangle$ and the $|2\rangle$ to $|3\rangle$ transitions, the hyperfine splitting leads to relatively large inhomogeneous broadening such that $\tau_{13} = \tau_{23} \approx T_2^* = 18$ ms [17]. This corresponds to a Rabi linewidth of 33 Hz for the hyperfine transitions.

Figure 2 shows a typical $M1$-CPT line shape when the trapping field is linearly polarized, $|\Omega| = 2\pi \times 250$ Hz, and $1/R = 5.8$ ms. For the measurement, ω_p is scanned while ω_q is fixed to the $|2\rangle$ to $|3\rangle$ resonance including the ac-Stark shift $\delta_3 = 2\pi \times 400$ Hz. The optical and the rf fields are applied for 250 ms, which is long enough to establish a steady state, to the atoms in the $|1\rangle$ state. After the fields are turned off, the three populations are measured one at a time, and the measurements are repeated three times. In Fig. 2, the fractional populations ρ_{11}, ρ_{22}, and ρ_{33} are denoted by black squares, red circles, and blue triangles, respectively. The lines are the
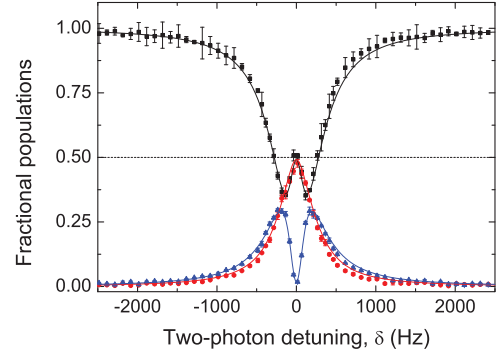
FIG. 2. (Color online) Line shape of $M1$ CPT. Fractional populations of ρ_{11} (black squares), ρ_{22} (red circles), and ρ_{33} (blue triangles) are shown. The lines are the steady-state solutions of the density-matrix equations, Eqs. (1). $|\Omega_p| = |\Omega_q| = 2\pi \times 250$ Hz, $1/R = 5.8$, $1/\gamma_{12} = 650$, $1/\gamma_{13} = 650/9$, and $1/\gamma_{23} = 650/4$ ms.

steady-state solutions of Eqs. (1) without a convolution. There is no fitting parameter and the agreement is excellent. Because the inhomogeneous broadening of 33 Hz is smaller than the dark resonance linewidth of 130 Hz, the convolution does not have a noticeable effect. At the steady state,

$$\rho_{33} = \frac{2}{(p_1 + p_2)R} [\Omega_p \operatorname{Im}(\rho_{13}) + \Omega_q \operatorname{Im}(\rho_{23})], \tag{3}$$

and ρ_{33} is closely related to a weighted absorption coefficient of the rf fields.

At $\delta = 0$, $\rho_{33} = 0$ and $\rho_{11} = \rho_{22} = 1/2$, thereby implying complete pumping to the dark state, which has the form $|\Psi_{\text{CPT}}(t)\rangle = (e^{-i\omega_1 t}|1\rangle + e^{-i\omega_2 t + i\phi}|2\rangle)/\sqrt{2}$, where ϕ is a phase difference. Using the $M1$ interaction driven by Ω_p and Ω_q, $H_{\text{M1}} = \hbar(\Omega_p e^{-i\omega_p t}|3\rangle\langle 1| + \Omega_q e^{-i\omega_q t}|3\rangle\langle 2|) + \text{H.c.}$, $\phi = \pi$ when $\Omega_{p,q}$ are real [3]. In order to measure ϕ, we turn off $\vec{E}_c$ and apply a $\pi/2$ pulse of an SRT between $|1\rangle$ and $|2\rangle$ to the dark-state atoms. We use the rf fields satisfying the conditions in Eqs. (2) with ($m = 0, n = 1$) and with the $\vec{B}_q(t)$ phase shifted by θ. The transition probabilities to the $|1\rangle$ and $|2\rangle$ states are $[1 + \sin(\phi - \theta)]/2$ and $[1 - \sin(\phi - \theta)]/2$, respectively. The results in Fig. 3 confirm that $\phi = \pi$. We also study the evolution of the atoms in $|1\rangle$ toward the steady
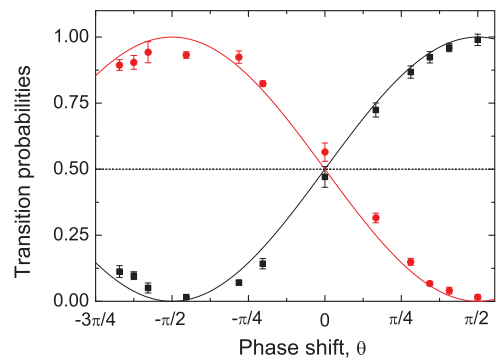
FIG. 3. (Color online) Transition probabilities from the CPT dark state $|\Psi_{\text{CPT}}(t)\rangle = (e^{-i\omega_1 t}|1\rangle + e^{-i\omega_2 t + i\phi}|2\rangle)/\sqrt{2}$ to the $|1\rangle$ state (black squares) and the $|2\rangle$ state (red circles). The stimulated Raman transition is driven by $\vec{B}_p(t)$ and $\vec{B}_q(t)$ with the phase of $\vec{B}_q(t)$ shifted by θ.
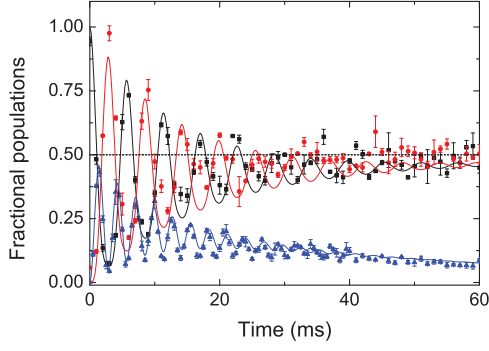
FIG. 4. (Color online) Evolution of the atoms in the $|1\rangle$ state toward the CPT dark state. Fractional populations of $\rho_{11}(t)$ (black squares), $\rho_{22}(t)$ (red circles), and $\rho_{33}(t)$ (blue triangles) are shown. The lines are the time-dependent solutions of Eqs. (1). Experimental parameters are the same as those in Fig. 2 with $\delta = 0$.

state at $\delta = 0$ of Fig. 2. Figure 4 shows $(\rho_{11}(t), \rho_{22}(t), \rho_{33}(t))$ at an interval of 1 ms. The lines represent the time-dependent solutions of Eqs. (1).

Finally, we measure the CPT line shapes of ρ_{33} while either R or γ_{ij} is changed. $1/R$ is changed from 5.8 to 1.6 and 0.4 ms by increasing $\vec{E}_c$, and the results are shown in Fig. 5. They show close agreement with the theory curves. We note that while R affects the maximum value of ρ_{33} and thereby contrast of the CPT resonance, the minimum ρ_{33} is relatively independent of R. In order to change γ_{ij}, a calibrated white noise is injected to the Helmholtz-coil current, and τ_{12} is measured by Ramsey spectroscopy. Starting from $1/\gamma_{12} = 650$ ms without the injected noise, we set $1/\gamma_{12} = 36.3$ and 15.4 ms. γ_{13} and γ_{23} are inferred from the relations $\gamma_{13} = 9\gamma_{12}$ and $\gamma_{23} = 4\gamma_{12}$, respectively. The results for ρ_{33} are shown in Fig. 6, and the agreement is only qualitative. In each measurement of a Ramsey signal with an interrogation time t, while inhomogeneous broadening is averaged over the thermal distribution of atoms, homogeneous broadening results in an overall shot-to-shot fluctuation of the phase by $(\Delta\mu_B/\hbar) \int_0^t \delta B(t') dt'$. $\Delta\mu_B = (g_F m_F - g_{F'} m'_{F'})\mu_B$ with μ_B being the Bohr magneton. The Ramsey signal becomes fairly noisy and precise determination of the decoherence time constant is difficult.
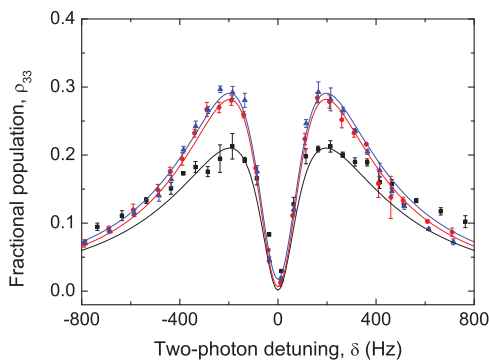
FIG. 5. (Color online) $M1$-CPT line shape vs the transition rate R. ρ_{33} in the steady state at $1/R = 5.8$ (blue triangles), 1.6 (red circles), and 0.4 ms (black squares) are shown with the corresponding solutions of Eqs. (1). The Rabi frequencies and γ_{ij} are the same as those in Fig. 2.
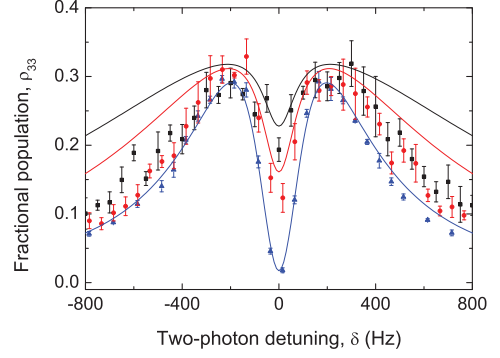
FIG. 6. (Color online) $M1$-CPT line shape vs the decoherence rate γ_{ij}. ρ_{33} in the steady state at $1/\gamma_{12} = 650$ (blue triangles), 36.3 (red circles), and 15.4 ms (black squares) are shown with the corresponding solutions of Eqs. (1) with $\gamma_{13} = 9\gamma_{12}$ and $\gamma_{23} = 4\gamma_{12}$. The Rabi frequencies and R are the same as those in Fig. 2.

IV. CONCLUSION

We constructed an ideal system to study coherent population trapping using a Λ configuration coupled by magnetic dipole interactions with a controllable optical pumping rate. By turning off the optical and the radio-frequency fields, the system can be frozen so that the quantum state of the medium can be probed precisely. Our system provides a closed Λ configuration and it can be used for a cooling mechanism for optically trapped atoms or for pumping atoms to a well-defined superposition state in a robust manner.

APPENDIX: REDUCTION OF THE FOUR-LEVEL INVERTED Y SYSTEM TO THE THREE-LEVEL Λ SYSTEM

The inverted Y system for $M1$ CPT is shown in Fig. 1(a). The energy eigenvalue of the $|j\rangle$ state is $\hbar\omega_j$ for $j = 1,2,3,4$. The $|4\rangle$ state has a spontaneous decay rate Γ_4 and all other states are stationary. The $(|1\rangle, |3\rangle)$ and $(|2\rangle, |3\rangle)$ states are coupled by magnetic dipole ($M1$) transitions and $(|3\rangle, |4\rangle)$ by an electric dipole ($E1$) transition. The $M1$ transitions are driven by rf fields $\vec{B}_j(t) = \vec{B}_j e^{-i\omega_j t} + \text{c.c.}$, where $j = p,q$. The Rabi frequencies are $\Omega_p = \langle 3| - \vec{\mu} \cdot \vec{B}_p |1\rangle/\hbar$ and $\Omega_q = \langle 3| - \vec{\mu} \cdot \vec{B}_q |2\rangle/\hbar$, where $\vec{\mu}$ is a magnetic dipole moment operator. The $E1$ transition is driven by an optical field $\vec{E}_c(t) = \vec{E}_c e^{-i\omega_c t} + \text{c.c.}$, and the Rabi frequency is $\Omega_c = \langle 4| - \vec{d} \cdot \vec{E}_c |3\rangle/\hbar$. $\vec{d}$ is an electric dipole moment operator. The interaction Hamiltonian is

$$H_{\text{int}}(t) = \hbar(\Omega_p e^{-i\omega_p t}|3\rangle\langle 1| + \Omega_q e^{-i\omega_q t}|3\rangle\langle 2|$$
$$+ \Omega_c e^{-i\omega_c t}|4\rangle\langle 3|) + \text{H.c.} \quad \text{(A1)}$$

From the master equation,

$$\frac{d\rho}{dt} = -\frac{i}{\hbar}[H_{\text{int}}, \rho] + \left(\frac{\partial\rho}{\partial t}\right)_{\text{int}}, \quad \text{(A2)}$$

where the second term represents various damping processes, the density matrix equations in the interaction picture using the rotating wave approximation are given as follows [9]:

$$\dot\rho_{11} = i\Omega_p(\rho_{13} - \rho_{31}) + p_1\Gamma_4\rho_{44}, \tag{A3a}$$

$$\dot\rho_{22} = i\Omega_q(\rho_{23} - \rho_{32}) + p_2\Gamma_4\rho_{44}, \tag{A3b}$$

$$\dot\rho_{33} = -i\Omega_p(\rho_{13} - \rho_{31}) - i\Omega_q(\rho_{23} - \rho_{32})$$
$$+ i\Omega_c(\rho_{34} - \rho_{43}) + p_3\Gamma_4\rho_{44}, \tag{A3c}$$

$$\dot\rho_{44} = -i\Omega_c(\rho_{34} - \rho_{43}) - \Gamma_4\rho_{44}, \tag{A3d}$$

$$\dot\rho_{12} = -i\Omega_p\rho_{32} + i\Omega_q\rho_{13} - (i\delta + \gamma_{12})\rho_{12}, \tag{A3e}$$

$$\dot\rho_{13} = i\Omega_p(\rho_{11} - \rho_{33}) + i\Omega_q\rho_{12} + i\Omega_c\rho_{14}$$
$$- (i\Delta_p + \gamma_{13})\rho_{13}, \tag{A3f}$$

$$\dot\rho_{23} = i\Omega_p\rho_{21} + i\Omega_q(\rho_{22} - \rho_{33}) + i\Omega_c\rho_{24}$$
$$- (i\Delta_q + \gamma_{23})\rho_{23}, \tag{A3g}$$

$$\dot\rho_{14} = -i\Omega_p\rho_{34} + i\Omega_c\rho_{13} - [i(\Delta_c + \Delta_p) + \Gamma_4/2]\rho_{14}, \tag{A3h}$$

$$\dot\rho_{24} = -i\Omega_q\rho_{34} + i\Omega_c\rho_{23} - [i(\Delta_c + \Delta_q) + \Gamma_4/2]\rho_{24}, \tag{A3i}$$

$$\dot\rho_{34} = -i\Omega_p\rho_{14} - i\Omega_q\rho_{24} + i\Omega_c(\rho_{33} - \rho_{44})$$
$$- (i\Delta_c + \Gamma_4/2)\rho_{34}. \tag{A3j}$$

$\dot\rho_{ij} = \dot\rho_{ji}^*$ when $i \neq j$. $p_1, p_2,$ and p_3 are the branching ratios for the decays from $|4\rangle$ to $|1\rangle$, $|2\rangle$, and $|3\rangle$, respectively. $\Delta_p = \omega_p - (\omega_3 - \omega_1)$ and $\Delta_q = \omega_q - (\omega_3 - \omega_2)$ are the single-photon detunings and $\delta = \Delta_p - \Delta_q$ is the two-photon detuning. $\Delta_c = \omega_c - (\omega_4 - \omega_3)$ is the detuning of the coupling field. γ_{ij} is the decay rate of the coherence ρ_{ij}.

First we note that the spontaneous decay rate Γ_4 is much larger than the Rabi frequencies $\Omega_{p,q}$. This implies that the population ρ_{44} and coherence ρ_{34} reach steady states almost instantaneously, and consequently we may consider the two-level system ($|3\rangle$, $|4\rangle$) separately from $|1\rangle$ and $|2\rangle$ to obtain ρ_{44} and ρ_{34}. Under this situation,

$$\rho_{44} = \frac{R}{\Gamma_4}\rho_{33}, \tag{A4a}$$

$$\rho_{34} = \Omega_c \frac{\Delta_c + i\Gamma_4/2}{\Delta_c^2 + \Gamma_4^2/4}\rho_{33}, \tag{A4b}$$

where

$$R = \frac{|\Omega_c|^2}{\Delta_c^2 + \Gamma_4^2/4}\Gamma_4. \tag{A5}$$

We assume that $|\Omega_c| \ll \Gamma_4$ and consequently $\rho_{44} \ll \rho_{33}$. Using the above results,

$$\dot\rho_{11} = i\Omega_p(\rho_{13} - \rho_{31}) + p_1 R\rho_{33}, \tag{A6a}$$

$$\dot\rho_{22} = i\Omega_q(\rho_{23} - \rho_{32}) + p_2 R\rho_{33}, \tag{A6b}$$

and $\rho_{11} + \rho_{22} + \rho_{33} = 1$.

While $\dot\rho_{12}$ in Eq. (A3e) is independent of the $|4\rangle$ state, $\dot\rho_{13}$ in Eq. (A3f) and $\dot\rho_{23}$ in Eq. (A3g) depend on $\dot\rho_{14}$ and $\dot\rho_{24}$, respectively. We note that ρ_{14} reaches a steady state at the rate of $\Gamma_4/2$ and we may use the steady-state solution,

$$\rho_{14} = \frac{i\Omega_c}{i(\Delta_c + \Delta_p) + \Gamma_4/2}\rho_{13} - \frac{i\Omega_p}{i(\Delta_c + \Delta_p) + \Gamma_4/2}\rho_{34}, \tag{A7}$$

where ρ_{34} is given in Eq. (A4b), to rewrite Eq. (A3f) as

$$\dot\rho_{13} = i\Omega_p(\rho_{11} - \rho_{33}) + i\Omega_q\rho_{12}$$
$$- [i(\Delta_p - \delta_3) + R/2 + \gamma_{13}]\rho_{13}. \tag{A8}$$

We assumed that $\Delta_c \gg \Delta_p$, which is the case in our experiment, and we neglected ρ_{44} in comparison with ρ_{33}. $\delta_3 = |\Omega_c|^2/\Delta_c$ is the ac-Stark shift of the $|3\rangle$ state due to the coupling field $\vec E_c$ upon the assumption that $\Delta_c \gg \Gamma_4$, which is also the case in our experiment. Using similar arguments for $\dot\rho_{23}$ and putting $\Delta_p' = \Delta_p - \delta_3$ and $\Delta_q' = \Delta_q - \delta_3$, Eqs. (A3f) and (A3g) can be written as

$$\dot\rho_{13} = i\Omega_p(\rho_{11} - \rho_{33}) + i\Omega_q\rho_{12} - (i\Delta_p' + R/2 + \gamma_{13})\rho_{13}, \tag{A9a}$$

$$\dot\rho_{23} = i\Omega_p\rho_{21} + i\Omega_q(\rho_{22} - \rho_{33}) - (i\Delta_q' + R/2 + \gamma_{23})\rho_{23}. \tag{A9b}$$

Equations (A6a) and (A6b), (A9a) and (A9b), and (A3e) constitute the effective density matrix equations for the $M1$-CPT system in Fig. 1(b).

---

[1] G. Alzetta, A. Gozzini, L. Moi, and G. Orriols, Nuovo Cimento B **36**, 5 (1976).

[2] E. Arimondo, Prog. Opt. **35**, 257 (1996).

[3] R. Wynands and A. Nagel, Appl. Phys. B **68**, 1 (1999).

[4] J. Vanier, Appl. Phys. B **81**, 421 (2005).

[5] E. Alipieva *et al.*, Proc. SPIE **5830**, 170 (2005).

[6] O. Schmidt, R. Wynands, Z. Hussein, and D. Meschede, Phys. Rev. A **53**, R27 (1996).

[7] W. Harshawardhan and G. S. Agarwal, Phys. Rev. A **58**, 598 (1998).

[8] A. Aspect, E. Arimondo, R. Kaiser, N. Vansteenkiste, and C. Cohen-Tannoudji, Phys. Rev. Lett. **61**, 826 (1988).

[9] J. Qi, Phys. Scr. **81**, 015402 (2010).

[10] M. R. Doery, R. Gupta, T. Bergeman, H. Metcalf, and E. J. D. Vredenbregt, Phys. Rev. A **51**, 2334 (1995).

[11] R. Dum, Phys. Rev. A **54**, 3299 (1996).

[12] A. V. Taichenachev, V. I. Yudin, V. L. Velichansky, A. S. Zibrov, and S. A. Zibrov, Phys. Rev. A **73**, 013812 (2006).

[13] J. Vanier, A. Godone, and F. Levi, Phys. Rev. A **58**, 2345 (1998).

[14] P. R. Hemmer, D. P. Katz, J. Donoghue, M. Cronin-Golomb, M. S. Shahriar, and P. Kumar, Opt. Lett. **20**, 982 (1995).

[15] J. M. Choi and D. Cho, J. Phys.: Conf. Ser. **80**, 012037 (2007).

[16] S. Kuhr, W. Alt, D. Schrader, I. Dotsenko, Y. Miroshnychenko, A. Rauschenbeutel, and D. Meschede, Phys. Rev. A **72**, 023406 (2005).

[17] H. Kim, H. S. Han, and D. Cho, Phys. Rev. Lett. **111**, 243004 (2013).

[18] H. Kim, H. S. Han, J. Park, Y. S. Kim, and D. Cho, Phys. Rev. A **88**, 061404(R) (2013).

[19] Z. Kim, S. Y. Kim, S. G. Lee, C. W. Kim, Q.-H. Park, and D. Cho, Rev. Sci. Instrum. **75**, 2752 (2004).